A Silicon Pad Detector for E-835 experiment at Fermilab

A. Buzzo [a] P. Musico [a] M. Pallavicini [b] C. Patrignani [b] E. Robutti [b]

[a] *INFN, Sezione di Genova, via Dodecaneso 33 I-16146 Genova, Italy*

[b] *INFN, Sezione di Genova e Università di Genova, via Dodecaneso 33 I-16146 Genova, Italy*

Abstract

We have built a Silicon Pad Detector for experiment E-835 at Fermilab.

The detector general features are: (a) compactness; (b) good resolution on the longitudinal track coordinate (along the beam); (c) capability of delivering pixel information; (d) full geometrical acceptance in the solid angle covered by the experiment; (e) good transparency; (f) fast multiplexed read out.

These characteristics will prove particularly effective to identify and reconstruct the $\Phi\Phi \longrightarrow 4K$ final state, thus allowing the experiment to study the elusive $^1P_1$ charmonium state in this decay channel too.

Preprint submitted to Elsevier Science *3 September 1997*

1 Introduction

The Silicon Pad Detector (SPD) is part of the E-835 inner tracking system. E-835 is the upgrade of the E-760 experiment ([1–6]), devoted to study charmonium spectroscopy at Fermilab.

To study the pseudoscalar states ($J^{PC} = 0^{-+}$) in E-760 the only available electromagnetic channel was the two photon one, which is affected by a large background coming from $\pi^0\pi^0$ and $\pi^0\gamma$ channels ([5]); in order to improve our experimental sensitivity on these states we are going to study them using the $\phi\phi$ channels as well, namely:

$$p\bar{p} \to \eta_c, \eta_c' \to \Phi\Phi \to K^+K^-K^+K^- \tag{1}$$

$$p\bar{p} \to^1 P_1 \to \eta_c\gamma \to \Phi\Phi\gamma \to \gamma K^+K^-K^+K^- \tag{2}$$

In order to handle the large particle flux (instantaneous luminosity will be higher than 3. $10^{31} cm^{-2}s^{-1}$ at the $^1P_1$ energy (3.526 MeV in $p\bar{p}$ c.o.m. frame) with an accepted rate around 5 MHz) and to achieve the desired spatial resolution of 2 $mrad$ in ϕ and 3 $mrad$ in θ (polar angle measured from the $\bar{p}$ direction which defines the z axis of our reference system) we decided to build a compact and large acceptance SPD, using a cylindrical geometry with internal radius 7.5 cm and external 10.0 cm. The detector covers 15 to 65 degrees in θ, 360 degrees in ϕ.

The pixel structure and the fast read out of the detector provide a powerful tool to disentangle the $\Phi\Phi$ candidates from the huge hadronic background using multiplicity and topological cuts, both simple and CPU time saving, which will be implemented in the third level software trigger. In fact, the tower structure of the SPD provides a quick way to correlate θ and ϕ measurements coming from other detectors.

This paper is structured as follows: section 2 describes the crystal geometry and their physical main features; in section 3 the front-end printed board design and crystal packing are shown; the whole detector mechanical structure and cooling system are outlined in section 4 while cosmic rays and beam tests results are given in section 5.

Feature	Value	Unit
Length	25.60±0.05	mm
Width	26.00±0.05	mm
Thickness	350±20	μm
Pad dimension	2.85x23.9	mm
Pads separation	0.1	mm
Active area	561.65	mm^2
Pad per crystal	8	-
Guard ring width	950	μm

Fig. 1. *Silicon crystals geometry and main features*

2 Silicon crystals

Crystal [1] geometrical dimensions have been dictated by physical and practical considerations in order to obtain the desired accuracy in the measurement of the z-coordinate (around 0.7 mm using both layers) and to keep their cost at an affordable level [2] but many other considerations have been taken into account as well: a) the total surface to be covered (about 2000 cm^2 with two layers); b) the easiness in manipulating and mounting/dismounting the crystals on the PCB; c) the diode capacitance; d) the total cost.

All these requirements have led us to choose the geometrical dimensions shown in Figure 1.

Each detector is $25.6 \times 26.0 \times 0.350\ mm^3$ and is surrounded by a 0.950 mm wide guard ring which prevents bulk and surface currents to go into the DC coupled amplifier inputs.

This guard ring reduces the active area of each detector to 561.7 mm^2 (total area 665.6 mm^2) but improves its performance by dramatically reducing the noise coming from leakage current fluctuations. Guard ring design is based on references [9]-[10] and is optimized to keep pad currents around a few nA (maximum a few tens) even at temperature around 40-50 degrees Celsius.

To choose the appropriate thickness for the crystals we had to trade off between

[1] Manufacturer: SINTEF,Postboks 124 Blindern,N-0314 Oslo,NORWAY

[2] Silicon processing is done on circular wafers whose diameter is (in our case) 101.6 mm; using rectangular crystals, geometry should be chosen to inscribe exactly a few of them in a circle in order to reduce scraps.

the experimental request to have very small thickness and our need to reduce diode capacitance at the amplifier inputs, thus achieving a good signal/noise ratio: with 350 μm detectors the total radiation length seen by a particle traversing the crystal at 90 degrees is around 0.004 X_0, less than 20% of the total thickness and the diode capacitance is around 25 pF, a value small enough to obtain for our amplifier a confortable equivalent input noise of about 1500 electrons r.m.s.

The back side of the crystal is covered with an aluminium layer (thickness 20 μm) which allows to supply a positive bias voltage to the diodes. This solution has been mostly dictated by the lack of space for the capacitors we should have put in if we had used a negative bias on the pads.

Depletion voltage, guard ring current and pad currents have been carefully measured for each detector in order to gather on the same module crystals with similar depletion voltage [3] and to identify and reject bad ones; results are shown in Figure 2.

We note, in particular, that the crystals are divided in two main groups, one with full depletion voltage around 30 V, the second around 60 V. This fact, due to two different doping concentration in the n-type substrate, has no measurable effect on detection efficiency (see section 5).

The estimated fluence of minimum ionizing particles crossing one cm^2 of the detector during the whole data taking is around 10^{12}, therefore we do not expect a big increase in pads currents due to radiation damage.

3 Printed board

Each module of the detector is built on a Printed Circuit Board (PCB) 1.0 mm thick, 34.0 mm wide and 380 mm long (or 390 mm) [4]; the PCB has three layers of G-10, 200 μm thick, each of them with two layers of copper for electrical connections.

Front-end electronics (on one side) and the double layer of silicon detectors (on the other side) are both set on the PCB, as shown in Figure 3 (a). The PCB weight, excluding electronic components and silicon detectors, is 33.5 g

[3] On each module (see section 3) 24 crystals are biased by the same line: crystals with very different depletion voltage would be either inefficient because of their incomplete depletion or noisy

[4] There are circuits of two different length to reduce interference between connectors in the downstream end of the detector but the active area and the geometry of the crystals mounted on them is exactly the same for both types

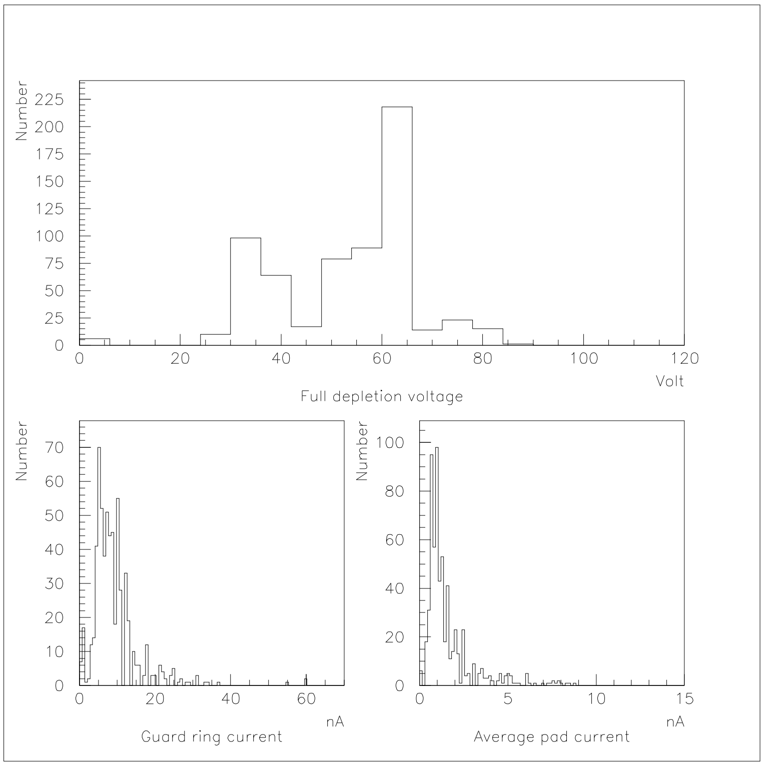

Fig. 2. *Crystal measurement results for the whole sample of 630 detectors. Upper plot is the full depletion voltage distribution, which shows a two peak structure, due to two different doping concentrations in the n-type substrate. Lower plots are the guard-ring current distribution and the pad current distribution (average over 8 pads).*

(short) and 35.0 g (long), corresponding to a 90 degrees radiation length of 0.008 X_0, mainly due to copper layers.

After soldering all electronics and connector the total weight reaches 54.5 g (short) and 56.0 g (long). The estimated averaged total radiation length (including silicon crystals) becomes 0.028 X_0, giving a ratio between active material thickness and total thickness around 1 : 3.5

To make each module rigid enough and self-supporting, two G-10 walls (0.5 mm thick, 7 mm wide, 350 mm long) are glued to the PCB as shown in Figure 3 (a).

The following two sections give a brief description of the PCB structure and of the front-end electronics. A detailed one can be found in [7].

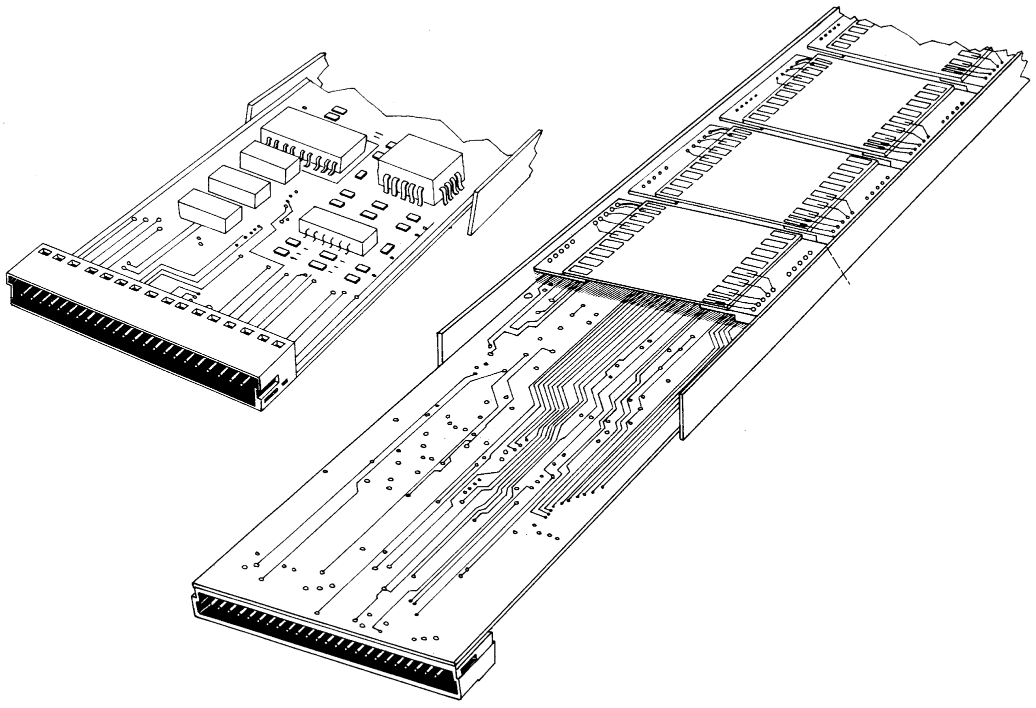

(a)

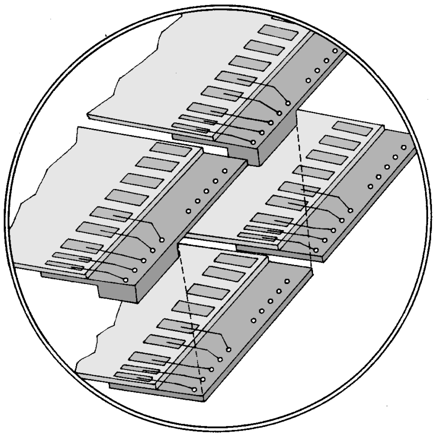

(b)

Fig. 3. *This pictures show the structure of one SPD module (slab); (a) shows the two faces of one PCB seen from the connector side; G-10 walls, electronic components and silicon crystal are shown as well; (b) shows a magnified view of the crystal side.*

3.1 *Silicon detectors layout*

Silicon diode detectors are arranged on one side of the PCB in two layers of 12 crystals each staggered by 13 mm (half a crystal) along the z coordinate in order to eliminate inefficiencies due to the geometrical crack (0.3 mm) between two crystals; each detector is glued to two small G-10 circuits (0.5 $mm \times 5.5$ $mm \times 26.0$ mm) that are attached to the PCB via 10 golden tungsten wires (diameter 100 μm).

All diodes are connected to the G-10 supports using the wire-bonding technique. One of the two G-10 support has a small copper pad that is used to supply the polarization voltage to the diodes through a drop of conductive glue [5] while 10 tungsten wires carry the bias voltage, the guard ring connection to ground and the 8 diodes signals. As shown in Figure 3 (b), all wires pass through appropriate holes [6] (diameter 0.5 mm) and are soldered to the other side.

To reduce inefficiencies due to bad connections, we chose to put two wire-bondings in each pad, using aluminium wires with diameter 20 μm.

The upper layer supports have a spacer 1.5 mm thick to keep crystals in the correct position and to avoid short cuts between the aluminium layer and lower layer's wire-bondings.

3.2 *Front-end electronics*

24 crystals are arranged on each PCB, therefore 192 independent channels must be read. It has not been possible to read out the whole number of channels in parallel because of lack of space for the cables; furthermore we could not read out the whole PCB serially because the total read out time would have not fit the experiment requirements (total read-out time around 35 μs for a 50 long-words event).

We chose to compromize between these two issues by using a 16 channels chip amplifier with analog multiplexed read-out produced by SSS [7], named ICAR16 (see [11]). Each ICAR16 (see Figure 5) can perform amplifying, shaping and track-and-hold of each input channel; the multiplexed analog read-out can be

[5] We have used the conductive glue EPO-TEK H20E (resistivity $10^{-4}\Omega cm$) and the non-conductive one EPO-TEK 353ND

[6] Holes pitch in the G-10 supports has been chosen to be able to use the same production mask for both layers.

[7] Smart Silicon System S.A., Avenue de Chailly 23, CH-1012 Lausanne, Switzerland

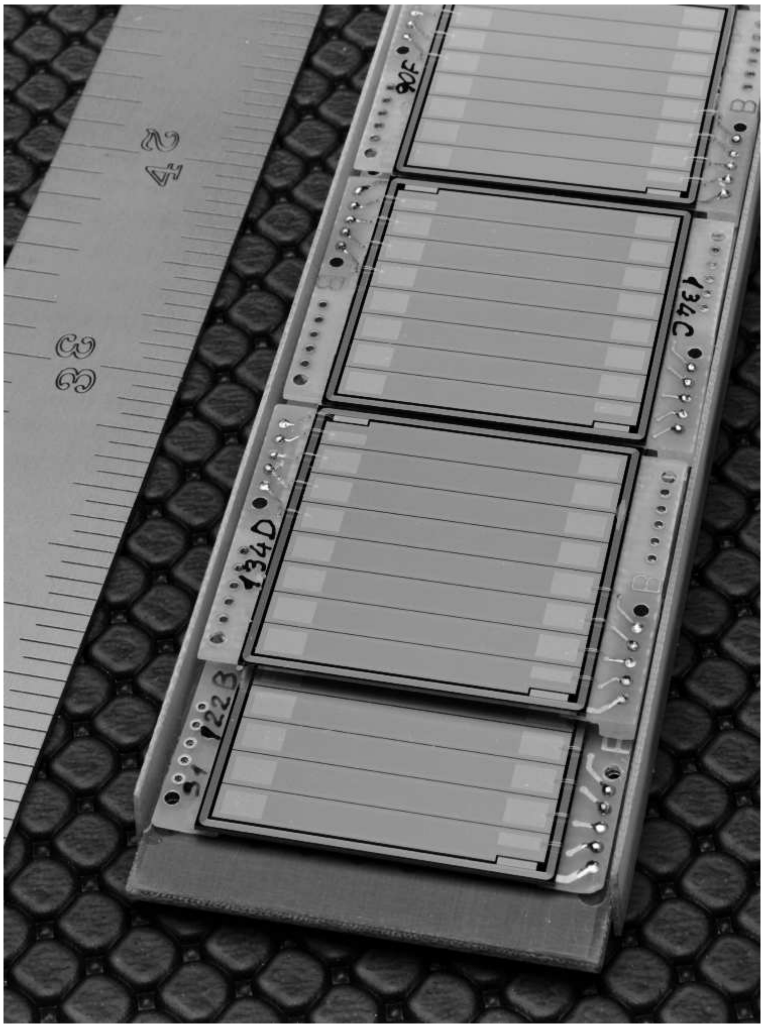

Fig. 4. *Magnified picture of the crystal side of a slab*

performed at a speed as high as 5 Mhz, giving a total read-out time of $3.2\mu s$.

12 ICAR16 chips are set on each PCB, to read out 192 channels. Figure 6 shows the block diagram of one read-out section: two silicon crystals (16 pads), one ICAR16 chip, one ECL comparator (Maxim MAX906), one DAC channel for the threshold (Analog Devices DAC-8800) and a buffer (Motorola MC34182) to drive the DAC output. The ICAR16 analog output signal is discriminated by an ECL-compatible voltage comparator. It should be noted that the comparator is triggered by a positive transition while ICAR16 by a negative one, therefore the same signal can control both devices taking into account the time response of ICAR16 output stage. Furthermore MAX906 output impedence is low enough to drive the 5 m twisted-pair line needed to deliver its output signal to the VME read-out electronics, so no additional driver is required.

All ECL digital signals that control ICAR16 (Track & Hold level, Chip Se-

Parameters	Min	Typical	Max	Unit
Power				
V_{ref}	-2.25	-2.5	-3.25	V
V_{ss}	-4.5	-5.0	-5.5	V
Current absorption				
Ground	-	17	34	mA
V_{ss}	-	-10	-20	mA
V_{ref}	-	-7	-14	mA
Gain	32	40	48	mV/fC
Peaking time	150	200	320	ns
Eq. input noise (C_{in} =**5** pF)	-	-	1000	e^-
Read out frequency	-	5	-	MHz

Fig. 5. *ICAR 16 main features*

lect level and multiplexing 5 MHz Clock) are supplied from the external[8] electronics [8].

All detecting diodes are DC connected to the amplifier inputs; due to a mistake in final ICAR16 production, a few nA steady current must be put into amplifier inputs through a resistor.

The 50-pin connector is set at one end of the PCB; all input and output signals are delivered through a flat cable plugged into this connector, except -5V power and ground because of the relatively high resistance of the wires[9].

The total power absorbed by one PCB is around 5 W (750 mA through -5V and 300 mA through +5V).

In order to be able to test both the front-end electronics and the connections of the diodes to the ICAR16 inputs, we put on the PCB two different test lines named T1 and T2; the former allows to inject a charge signal on the diodes through the bias line; the latter takes the charge signal directly to the ICAR16 input through a small capacitor built into the PCB from two small copper pads. These two circuits have shown up to be very useful to debug the

[8] Two MC10H116 triple line receivers are used to re-form all ECL signals
[9] Flat cable pitch is 0.635 mm and single wire resistance is around 2 Ω giving a voltage drop on -5V power around 1.5 V that, of course, cannot be tolerated

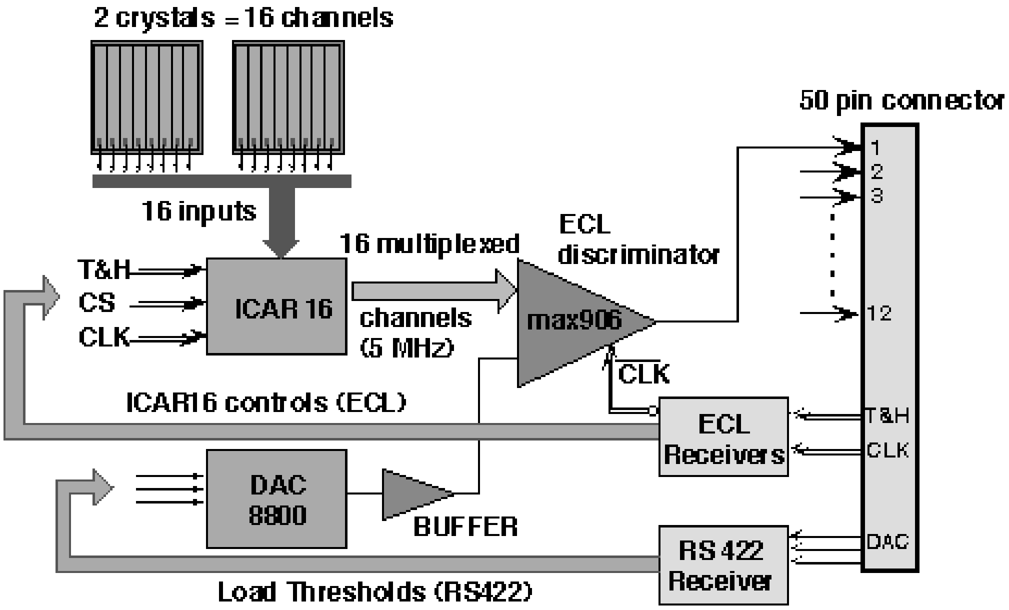

Fig. 6. *This picture shows a block diagram of one front-end electronics module; the main component ICAR 16 is shown together with two silicon crystals (16 channels), ECL discriminator and a DAC for the threshold (with a buffer); ECL receivers for ICAR16 control signals and RS422 receivers for thresholds loading are also shown.*

system and to find out bad components or connections.

Figure 7 shows the output waveform from an ICAR16, taken by a digital scope during a characterization test we made at a CERN beam line. The particle signal is clearly visible out of the other 15 empty channels in one multiplexing cycle.

4 Mechanical structure

As already said in section 1, we chose to build a cylindric shape detector in order to match the existing detector geometry. The structure is shown in Figure 8 together with part of the hydrogen jet target to which the detector is hung.

The 24 modules are arranged in a double layer barrel geometry with a carbon fiber cylinder and two G-10 flanges to support the whole structure (see Figure 9). The 12 short modules are mounted at a radius of 8.15 cm while long modules are set at radius 9.05 cm. The overlap in azimuth acceptance of the two layers is around 0.5 degrees to avoid inefficiencies due to misalignment. The support cylinder is 0.6 mm thick, has internal radius 75.5 mm and is 403 mm long.

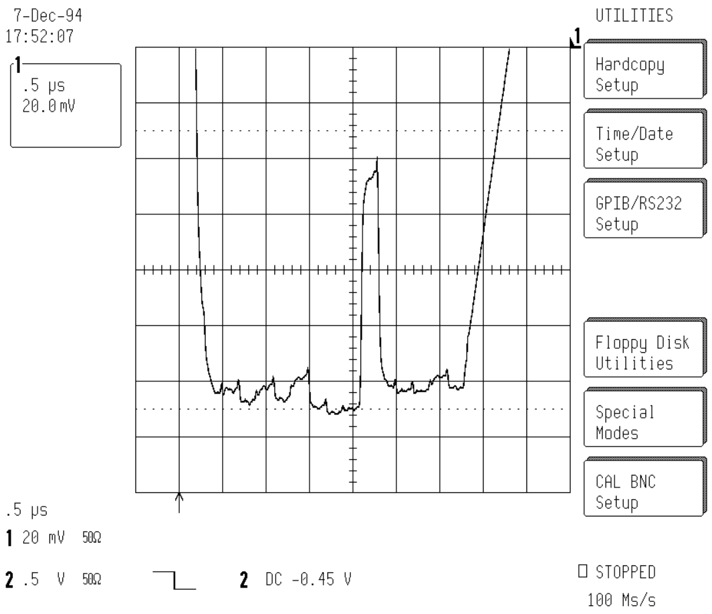

Fig. 7. *ICAR16 output waveform triggered by a minimum ionizing particle; this picture has been taken by a digital scope (Le Croy ScopeStation 140) triggered by the coincidence of three scintillators aligned with the detector. The analog multiplexed signal is 3.2 μs, corresponding to 16 channels at 5 MHz. The pad connected to ICAR16 channel 11 has been hit by a 5 GeV/c pion, while the other 15 ICAR channels show only noise.*

The first flange has been built from a single G-10 piece 5 mm thick and can support the whole cylinder through 4 screws; also mounted on the flange are 6 gas inlets (8 mm diameter) to provide the cooling air flow. The second flange keeps the 24 circuits in the correct position. Both flanges are glued to the carbon fiber cylinder to form a reel shape support.

The whole cylinder is then closed by a G-10 sheet (0.1 mm thick), whose external face is covered with a thin layer of carbon paint, in order to protect it from light and dust and to provide a shield from external electromagnetic noise (both internal and external cylinder are grounded).

The total SPD weight is 2.2 Kg excluding read-out cables; the 90 degrees estimated radiation lenght amounts to 0.035 X_0 [10]

As we said in section 3, power dissipated by one single PCB is above 5 W, giving a total absorption of about 130 W. Silicon detector performance is badly spoiled at high temperature, so a suitable cooling system must be provided. In order to minimize non active material inside detector acceptance, we decided not to use a refrigerating liquid. Gas cooling is enough to achieve a working temperature around 35 degrees Celsius using a gas flow about 3.5 l/s with an

[10] Detector thickness is not uniform at all and depends both on θ and ϕ; thickness ranges between 0.020 X_0 and 0.045 X_0 giving the smeared value quoted in the text.

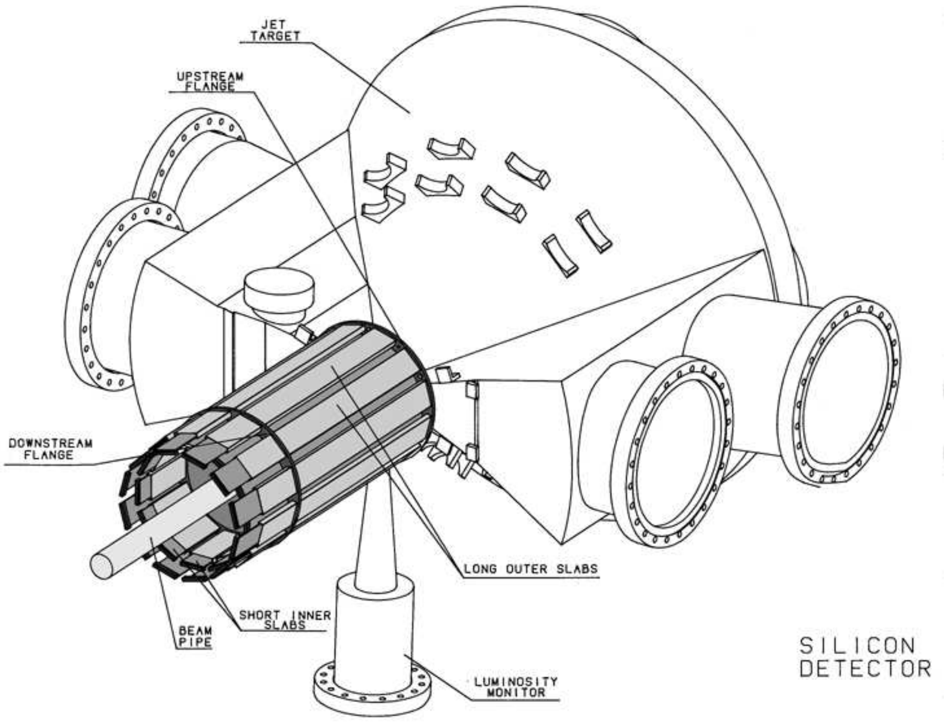

Fig. 8. *Picture view of the Silicon Pad Detector and part of the jet target to which the detector is hung; inner and outer slabs are clearly visible together with the inner support cylinder, the two G-10 flanges and part of the beam pipe; this picture does not show the outer G-10 sheet that covers the whole cylinder and flat cables that must be plugged to the downstream connectors.*

input temperature around 15 degrees. In principle nitrogen would have been the best choice but practical and cost concerns have led us to use a clean and dry air flow.

5 Cosmic rays and test beam results

The SPD has been tested both using cosmic rays and a 5 $GeV/c\,\pi^-$ beam in two different periods at the CERN Hall East (a prototype with just two crystals during november 1994 and 50% of the whole detector in october/november 1995).

The first beam test was devoted to study detector response to minimum ionizing particles and to measure its signal/noise ratio; to have a deeper insight into detector performance, we decided to use an analog read-out based on a digital scope together with the digital read-out [11] .

[11] On each slab the output signal of one single ICAR16 (out of 12) is also connected

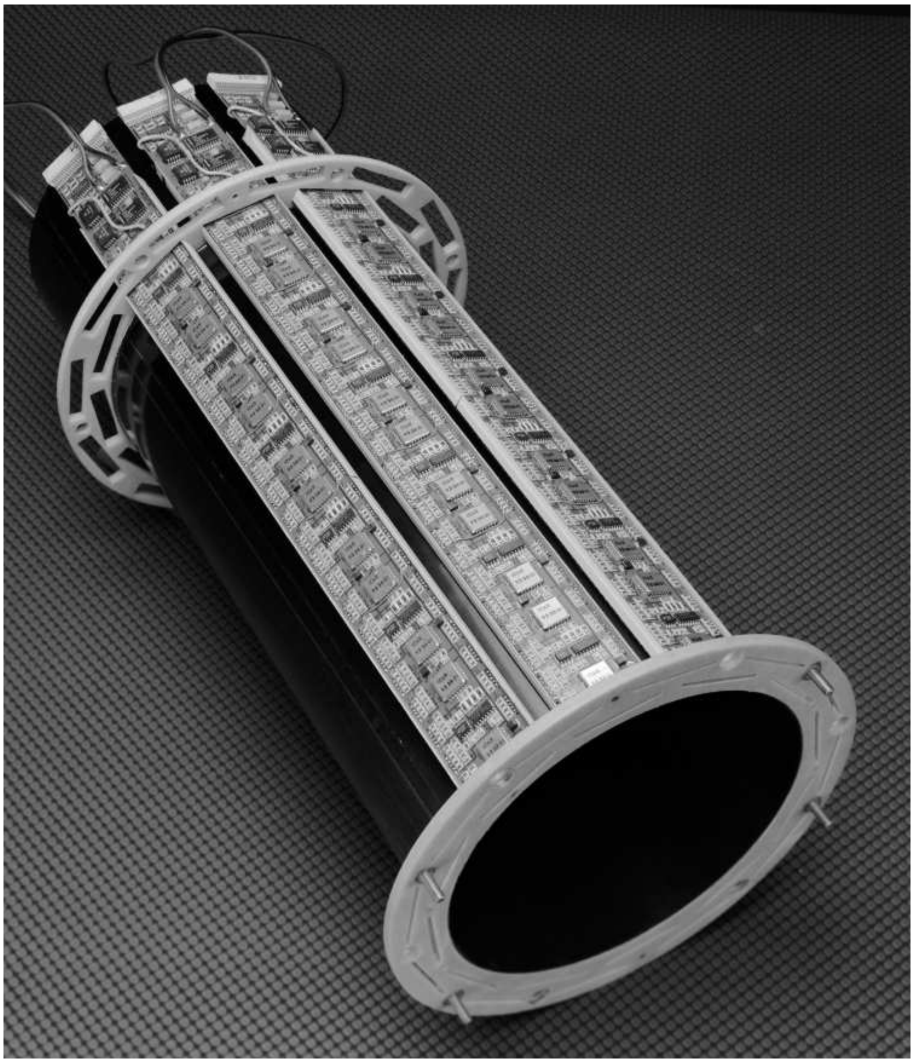

Fig. 9. *The carbon fiber support with three inner slabs (short type) already mounted; the two G-10 flanges are clearly visible together with the power supply twin cables. Flat cables for signals and controls are not shown.*

In this way we could read out about 1000 ICAR16 waveforms triggered by minimum ionizing particles, which have been used to study detector response. An example of these waveforms is shown in Figure 7 where the signal due to a charged particle traversing the crystal at 90 degrees is clearly visible together with 15 small spikes due to other empty channels .

Figure 10 shows the S/N ratio as a function of Track & Hold delay, being $\Delta t = 0$ at the particle crossing time; the best performance is achieved with $\Delta t = 300\ ns$ where S/N $\simeq 15$ [12].

---

to an analog driver and delivered to the external read-out electronics for test and monitoring.

[12] The Track & Hold delay dependence of the S/N ratio is quite obvious but it is very critical in our experiment; being set in a DC collider we have no time information

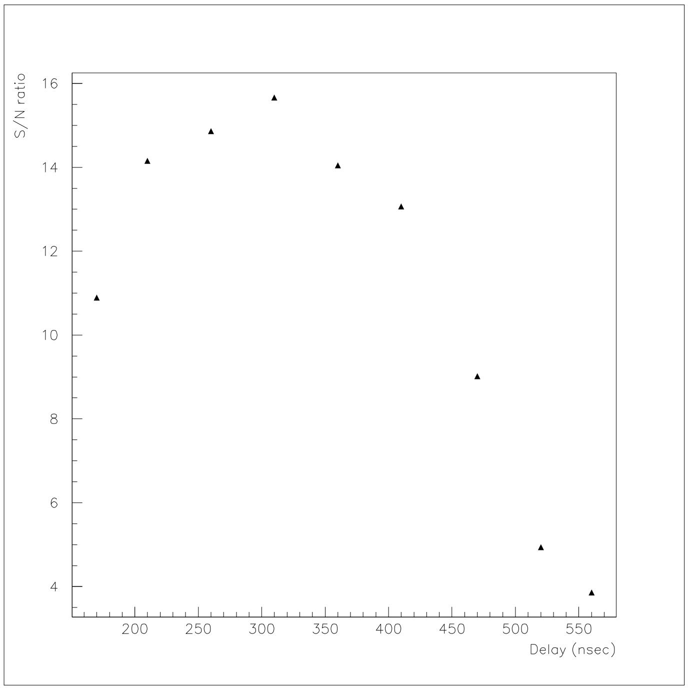

Fig. 10. *Signal / Noise ratio measured as a function of Track and Hold delay with respect to particle crossing time.*

The second beam test was meant to measure detector efficiency, position resolution and noise in operating condition similar to those we will have in E-835 experiment, using a statistically significant sample of channels (50% of the whole detector, 2304 channels). We set a tower of 12 slabs on the T10 test beam, using 3 "finger" scintillators as a trigger. About 10^6 minimum ionizing particle events have been recorded, with different thresholds and bias voltage in order to optimize these parameters and find the best operating conditions. To set the proper thresholds we first performed a scan, reading out 500 times the whole detector with different thresholds starting from values well below the ICAR16 DC output level and going well above; in this way a curve similar to the one shown in Figure 11 is obtained for each channel; by fitting this curve with the function:

$$C(V) = 1 - erf(\frac{V-\mu}{\sigma}) \tag{3}$$

we can measure both the average DC value and noise standard deviation with good accuracy. The result shown in figure 11 is $\sigma = 0.009V$ corresponding to an equivalent input noise of 1850 e^-.

Figure 12 shows the same plot as obtained with the pion beam on; in this

about the beam crossing, so we have to use the first level trigger to strobe the detector; the result shown in Figure 10 is very important because 300 ns is just what the trigger system needs to process the signals and strobe good events.

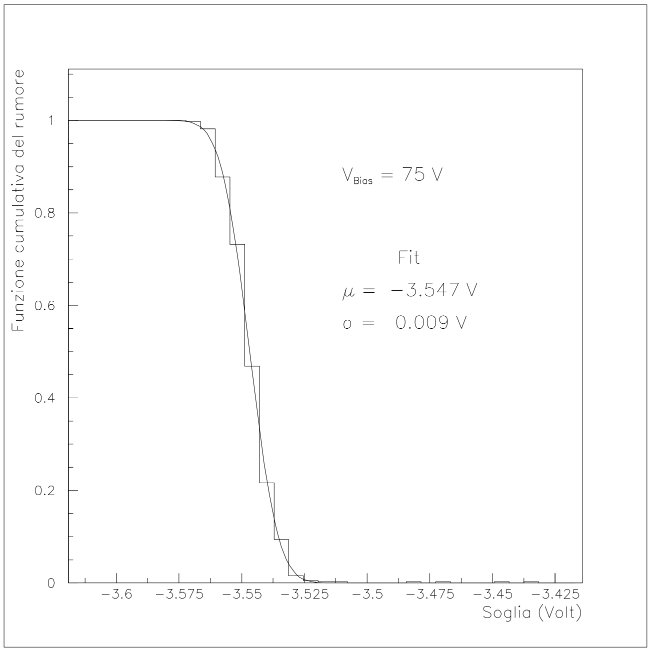

Fig. 11. *This plot shows the result of a threshold scan performed with beam off (pure noise); the vertical axis is the number of times the channel is ON while the orizontal axis is the threshold measured in V. The curve is the C(V) function defined in section 5 while the numbers shown are the fit results. The equivalent input noise is 1850* e^-.

case the fit is done with a function that is the sum of C(V) function and an integrated Landau distribution, from which we got the measurement of the Signal/Noise ratio shown in Figure 10. When thresholds are set 4 or 5 σ above ICAR16 DC values, 98 % of the channels work fine; remaining 2% of the channels is still noisy because of two main reasons:

1) Some ICAR16 have non uniform output DC value; for we have one single threshold per ICAR16, sometimes it is not possible to take this thresholds above each channel without loosing efficiency on the others[13].
2) Some channels are always ON because of large diode current.

Being all crystals set on two layers, the overall effect of these noisy channels on the particle detection efficiency is small.

Figure 13 shows the fitted residual of beam tracks hitting one slab at an angle of 30 degreees; the resolution is what is expected with two layers of 2.9 mm wide pads (the number of two hits clusters is around 1% and gives no important contribution to geometrical resolution).

[13] We could not afford to reject all chips with non uniform DC output.

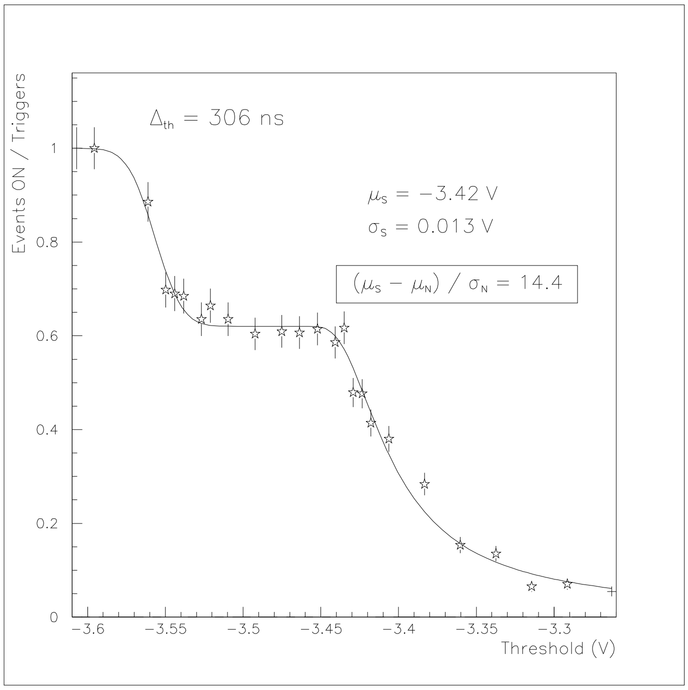

Fig. 12. *This plot shows the result of a threshold scan performed with beam on; the vertical axis is the number of times the channel is ON while the orizontal axis is the threshold in V. The curve is a C(V) function to fit the noise as in Figure 14 plus an integrated Landau distribution to include the contribution due to minimum ionizing particles.*

6 Acknowledgements

Many people have helped us to complete this project successfully.

The constant advice and encouragement by Prof. A. Santroni and Dr. M. Macrì were precious.

We are also deeply in debt with INFN technicians G. Barisone, S. Minutoli, M. Negri, P. Poggi who have contributed on detector design and have built it. We are also glad to acknowledge the work of G. Massari, M. Olcese, P. Pozzo on mechanical engineering and drawings and all people of the INFN mechanical workshop in Genova.

The work A. Bevilacqua and F. Siccardi on electronics design and testing is also acknowledged.

We also thank G. Darbo and L. Rossi (INFN Genova) for their useful advice.

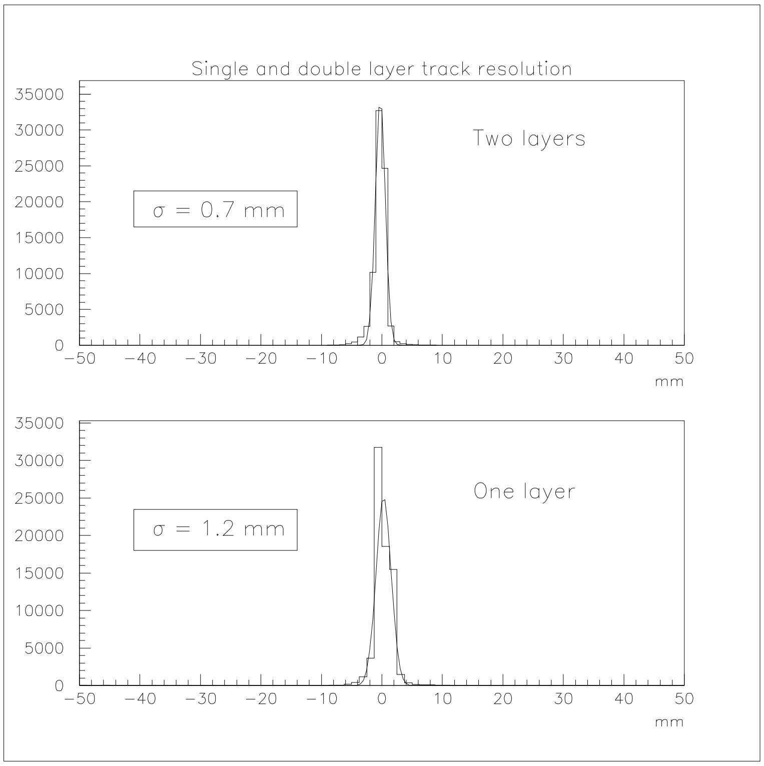

Fig. 13. *Spatial resolution for tracks hitting both layers of one slab at an incident angle of 30 degrees; upper plot is the resolution obtained using the information of both hits in the two staggered layers while lower plot shows the single pad resolution; the number of tracks which are associated to a cluster of hits in the same layer is negligible (around 1%) and gives no contribution to the resolution.*

References

[1] T.A. Armstrong et al., *Study of the χ_1 and χ_2 charmonium states formed in $\overline{p}p$ annihilations.* Nucl. Phys., **B373**(1992)35.

[2] T.A. Armstrong et al., *Measurement of the J/ψ and ψ' Resonance Parameters in $p\overline{p}$ Annihilations.* Phys. Rev. **D47**(1993)772.

[3] T.A. Armstrong at al., *Observation of the $^1P_1$ state of Charmonium.* Phys. Rev. Lett. **69**(1992)2337.

[4] T.A. Armstrong et al., *Measurement of the Proton Electromagnetic Form Factors in the Time-like Region at* 8.9 *to* 13.0 GeV^2. Phys. Rev. Lett. **70**(1993)1212.

[5] T.A. Armstrong et. al., *Study of the η_c (S wave singlet) state of charmonium formed in $\overline{p}p$ annihilations and a search for the η'_c* . Phys. Rev. **D52**(1995)4839.

[6] T.A. Armstrong et. al., *Study of the angular distribution of the reaction $\overline{p}p \rightarrow \chi_2 \rightarrow J/\psi\gamma \rightarrow e^+e^-\gamma$* Phys. Rev. **D48**(1993) 3037.

[7] M. Pallavicini, *Tesi di Dottorato di Ricerca in Fisica (Ph.D Thesis)* Genova University.

[8] P. Musico et. al., *The E835 Silicon Pad Detector DAQ System* (to be submitted to **NIM A**)

[9] L. Evensen et. al., *Guard ring design for high voltage operation of Silicon Detectors* Nucl. Instr. & Meth. **A 337** (1993) 44.

[10] L. Evensen et. al., *A fast low noise silicon detector for electron spectroscopy up to 1 MeV* Nucl. Instr. & Meth. **A 326** (1993) 136.

[11] P. Jarron et. al., *AMPLEX, a low noise, low power, analog CMOS signal processor for multi element silicon particle detectors* Proc. 5th European Symposium on Semiconductor Detectors
Munich, Germany, February 1989.